

## Solar G-band observations at Merak, Leh/Ladakh

N. Vasantharaju<sup>1</sup>, Namgyal Dorjey<sup>1</sup>, B. Ravindra<sup>1</sup>, K. Prabhu<sup>1</sup>, K. E. Rangarajan<sup>1,3</sup>, B. Prabhu Ramkumar<sup>1</sup> and K. Sankarasubramanian<sup>2</sup>

<sup>1</sup> Indian Institute of Astrophysics, Bengaluru

<sup>2</sup> Space Astronomy Group, ISRO Satellite Centre, Bengaluru

<sup>3</sup> Correspondences may be sent to this author

### Abstract

G-band observations are important for the study of dynamics of magnetic features in the solar photosphere and they are carried out using large telescopes, larger than 30 cm. We installed a 40 cm DFM telescope at one of the good sites (Ref: Site survey report submitted to Dept. of Science and Technology, India) in India; Merak in the district of Leh/Ladakh. We designed, fabricated and installed a back end instrument which involves a band-pass filter at G-band wavelength (430.5nm) to carry out observations of the solar photosphere on regular basis. In this paper, we report the installation of the telescope and the solar observations made with this back-end instrument. We present the details about the instrument used, data calibration and comparison with similar data obtained from space. We also discuss how the system can be improved for better quality images in the near future.

### Preamble

The observations of the Sun can be carried out in different wavelength bands of electromagnetic spectrum. On Earth, the observations of the Sun are made in optical, infrared and radio frequency regimes. In each of these wavelengths, different layers of the Sun are observed at different temperature and pressure. In the optical wavelength, it is possible to observe the solar photosphere and chromosphere. For coronal observations in the visible wavelength, specialized telescope – called coronagraph – is required. Indian Institute of Astrophysics has a history of observations of the Sun made in optical wavelengths using Kodaikanal observatory. Those observations are made in white light, Ca-K and H $\alpha$  wavelengths. Photosphere and chromosphere of the Sun are

sampled at these wavelengths. In many observatories around the world, photospheric observations are made in continuum of the blue/red CN-molecular and/or CH-molecular line. While the first one is sensitive to photospheric plasma, the later one provide good contrast for the magnetic features present in the photosphere. In many occasions, the observations made in CH-molecular line are used to study the dynamics of the magnetic features found in and around the sunspots as well as quiet regions (Berger et al. 1995; Ishikawa et al. 2007).

The G-band is a molecular band-head of the CH molecule. The wavelength of the band is  $430.54 \pm 0.5$  nm. The spectrum is observed because of the electronic transitions which also involve the vibrational and rotational levels. At low spectral resolution, the band-head looks like a single spectral line and Fraunhofer (1814) labeled the line by English letter " G" . The observations of the Sun made in G-band have very high contrast compared to that made in continuum. This is mainly due to the fact that CH molecule deplete through molecular dissociation in the deep photospheric layers of the flux tube atmospheres that is hot compared to the quiet sun surroundings. Rutten (1999) conjectured that CH molecule gets dissociated by the strong radiation field within the magnetic flux tubes. The photo dissociation of the CH molecule would reduce the line opacity within the tube producing a contrast enhancement.

Imaging in the G-band is commonly used to trace the small scale magnetic field concentrations (about 1500 G) of the Sun, although the mechanism that makes them bright has remained unclear. Images show conspicuous bright structures in the convective down flow regions (Muller & Roudier 1984; Muller 1985; Berger & Title 1996; Rutten et al. 2001; Langhans, Schmidt, & Tritschler 2002), where most of the concentrated magnetic flux is expected to reside (Weiss, Proctor, & Brownjohn 2002; Keller 1992; Dominguez Cerdena, Kneer, & Sanchez Almeida 2003). Much of our current knowledge about the structure, distribution, and dynamics of small-scale magnetic features is based on G-band observations under the assumption that G-band bright points represent magnetic flux concentrations and thus are often used as " proxies" for small scale magnetic elements (Berger et al. 1995,

1998; van Ballegooijen et al. 1998; De Pontieu 2002).

Indian Institute of Astrophysics (IIA) is planning to build a 2-m class solar telescope for the high resolution observations of the Sun. The telescope is planned to be put up in one of the three Himalayan sites where the effect of the Earth's atmosphere is small on the image distortion. Broad band imaging is one of the first light observations with the proposed telescope. G-band observations with this telescope are being planned. Also, in India nowhere G-band observations are made for the study of magnetic feature dynamics at the solar photosphere. To initiate such studies, a 40 cm telescope is installed at one of the sites, Merak, which is situated in Himalayan desert. This telescope was purchased for the purpose of Total solar eclipse observations and so the design was not optimized for G-band observations from Merak. Since eclipse observations are rare in the near future, as a test case, IIA has made it available for G-band studies from Merak. In this report we describe the design, fabrication, installation of the mechanical adapters used in the observations and the preliminary results. The next section is devoted for the details of the telescope, instrument and the detector. Later, we present the preliminary results of the observations. In the last section we discuss the improvement to the current instrument and plan for future routine observations of the Sun.

## **Telescope**

The G-band observations have been carried out using 40 cm classical Cassegrain with a primary mirror of F/3 and an effective focal ratio of F/5. The final focal length of the telescope is 200 cm. The field-of-view is about 87 arc min limited by Telescope tube structure. The focal plane position is between 1 and 20 cm from the instrument mounting surface with 11 cm being the nominal for F/5 beam. The telescope is of equatorial mount type. The telescope is supplied with control system for running the RA and Dec motors with a precision better than  $\pm 2$  arc sec in 2 minutes and better than  $\pm 15$  arc sec in one hour. It has built in software to control the telescope positions, speed and etc. More details about the telescope and control system can be obtained in the user manual provided by DFM Company, manufacturer of the telescope. The

final solar image size at the focal plane is about 18.6 mm which corresponds to a plate scale of 96.77 arc sec/mm.

### **Instrumentation**

The primary mirror of the telescope is 40-cm made out of zerodur material. The prolonged exposure of the primary mirror to the sunlight would heat up the mirror. With a 10% absorption it would be about 12 W of power absorbed. Convection would be set up within the telescope tube due to the heating up of primary and secondary mirror surfaces. Image quality would be affected with prolonged observations. To avoid the heating of the mirrors, we used 4 holes of size 5 cm in diameter placed at equal distance from the center of the aperture. This reduces the heat load on the primary mirror significantly. In order to reduce the heat further on the primary mirror we pasted four holes with a photo-film filter of density 3.8. The film filter cuts down the light intensity drastically and hence the heat load on the primary mirror. We used the film filter that has a same refractive index as that of air.

The main heart of the broad band imaging system is the G-band filter. It is primarily an interference filter with 2 cavities. The filter is centered at 430.54 nm and bandwidth of the filter is 0.84 nm. There is a slight change in the central wavelength position by a 0.01 nm as the ambient temperature changes by about 10 deg Celsius. As the pass-band of the filter is large, this change in the pass-band will not affect our observations.

The detector system used to detect the photons is the charge coupled device (CCD). The CCD has been acquired from PCO that has 2048×2048 pixels square array. The pixel size is 7.4 micron square. This is a front illuminated camera with a quantum efficiency of about 55% at a wavelength of 500 nm. The full well capacity is about 40000 electrons with a readout noise of about 9 electrons at 10 MHz readout rate. The camera can be cooled to -50 deg Celsius. The maximum number of frames can be obtained at its full resolution is about 15 frames per second.

The five cm size G-band filter has been housed in a circular ring. The circular ring has been kept in a large mount which is circular in shape

that can also hold the CCD camera. One side of the large mount is attached to the back end of the telescope and the CCD is attached on other side of it, between which the G-band filter is placed. The filter is kept in the converging beam and the CCD is kept in the focal plane. The length of the whole setup is about 20 cm.

The telescope is installed at 1.63 m above the ground level. The telescope mount height is about 0.5 m. Hence the primary mirror is located at a height of about 2.0 m above the ground. The telescope is polar aligned before starting the observations. The iron structure, telescope mount, the back end mount, filters position and the CCD position are shown in Figure 1. The four holes covered with the film filter can also be seen in Figure 1.



Fig-1. Main frame: The 16" classical Cassegrain telescope is installed at the shores of Pangong lake near Merak village on a robust platform at a height of about 1.63m from the ground surface. A high resolution PCO 2000 imaging camera (bluish in color) is also seen at its back end. Top right frame: PCO camera and its black anodized adapter. Middle right: Affixed 3.8 ND filter in the four holes of the aperture. Bottom

right: G-band filter is seen at back end of the scope.

## **Observations**

The telescope with the G-band filter was made operational at Merak in the month of July 2011. Firstly observations were made with Andor CCD camera of  $2k \times 2k$  format with pixel size 13.5 micron square. A full disk of the Sun was observed with this setup with a pixel resolution of 1.39 arc sec. Later in December 2011, to improve the spatial resolution we used a CCD camera from PCO which has a pixel size of 7.4 micron square. The PCO camera covers only the portion of the Sun with a pixel resolution of 0.76 arc sec. Using Nyquist criterion, we can definitely resolve structures greater than 1.5 arc sec. provided the other systems like filters and atmospheric seeing are of good quality. With this setup, we should be able to resolve big granules at least.

In December 2011, the observations have been made from 2<sup>nd</sup> December to 16<sup>th</sup> December. During this period the sky was normally good and we obtained data for about 3-4 hours at a cadence of 300 ms, 400 ms, 500 ms and 600 ms. There were some data gaps during the observations due to occasional passing clouds, image drift etc. A typical raw image obtained with the set up is shown in Figure 2. In the raw image, apart from the solar structures, some dust particles and streaks are also seen. These non solar structures are removed using the flat fielding.

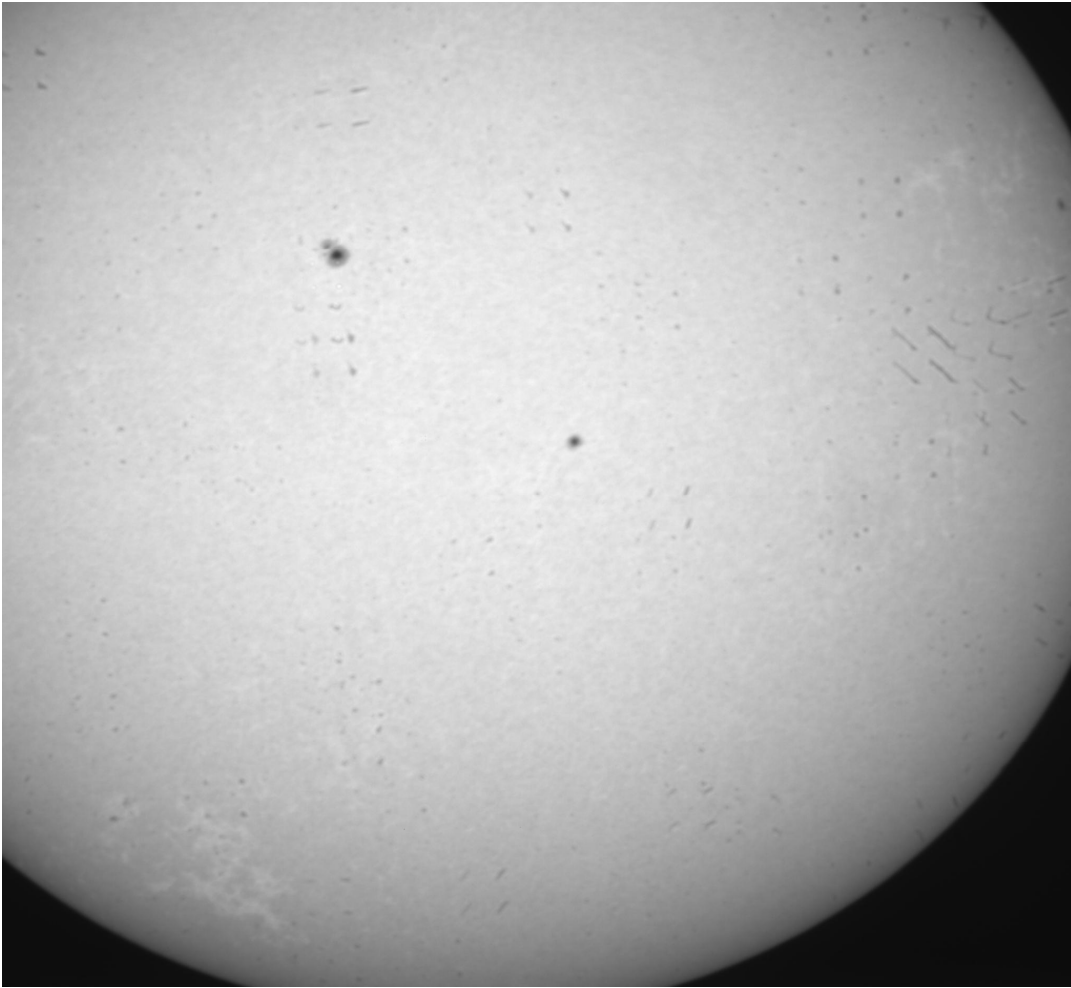


Fig-2: Raw image with exposure time 400 ms observed at Merak on 14 December, 2011 at 10:30 hrs

### **Calibration of G-band images**

We have taken the dark current image by covering the telescope aperture. The dark has been obtained before and after the solar observations. The flat fielding has been obtained by placing a diffuser in front of the telescope aperture. Many flat field frames were obtained and each flat is subtracted with the average dark. There was a small gradient in the averaged flat. This has been removed by fitting a polynomial to the 2-D surface. The resulting master flat field is normalized to the maximum count. The master flat is shown in Figure 3. The master flat field is used to calibrate the observed images. Each image in the time series is subtracted with the averaged dark current

and then divided by the master flat. The resulting image is shown in Figure 4. All the dust and non solar feature disappears once the flat fielding is done. Also, the contrast of the features increased. In Figure 4, apart from sunspot it is easy to identify the plages and small pores. Even the penumbra and umbra can be distinguished easily in sunspot structures.

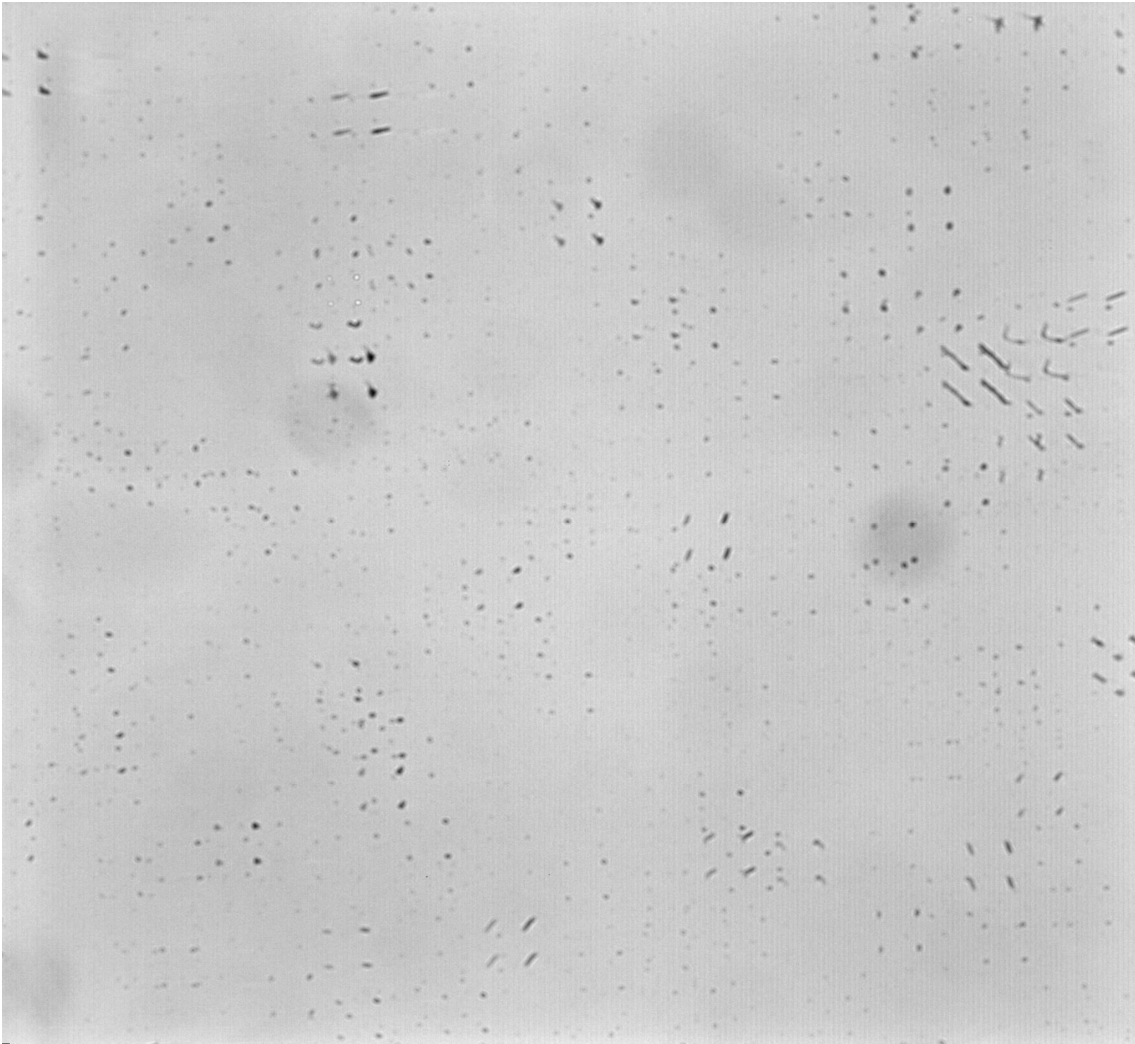


Fig-3: Normalized Master flat of exposure time 400ms



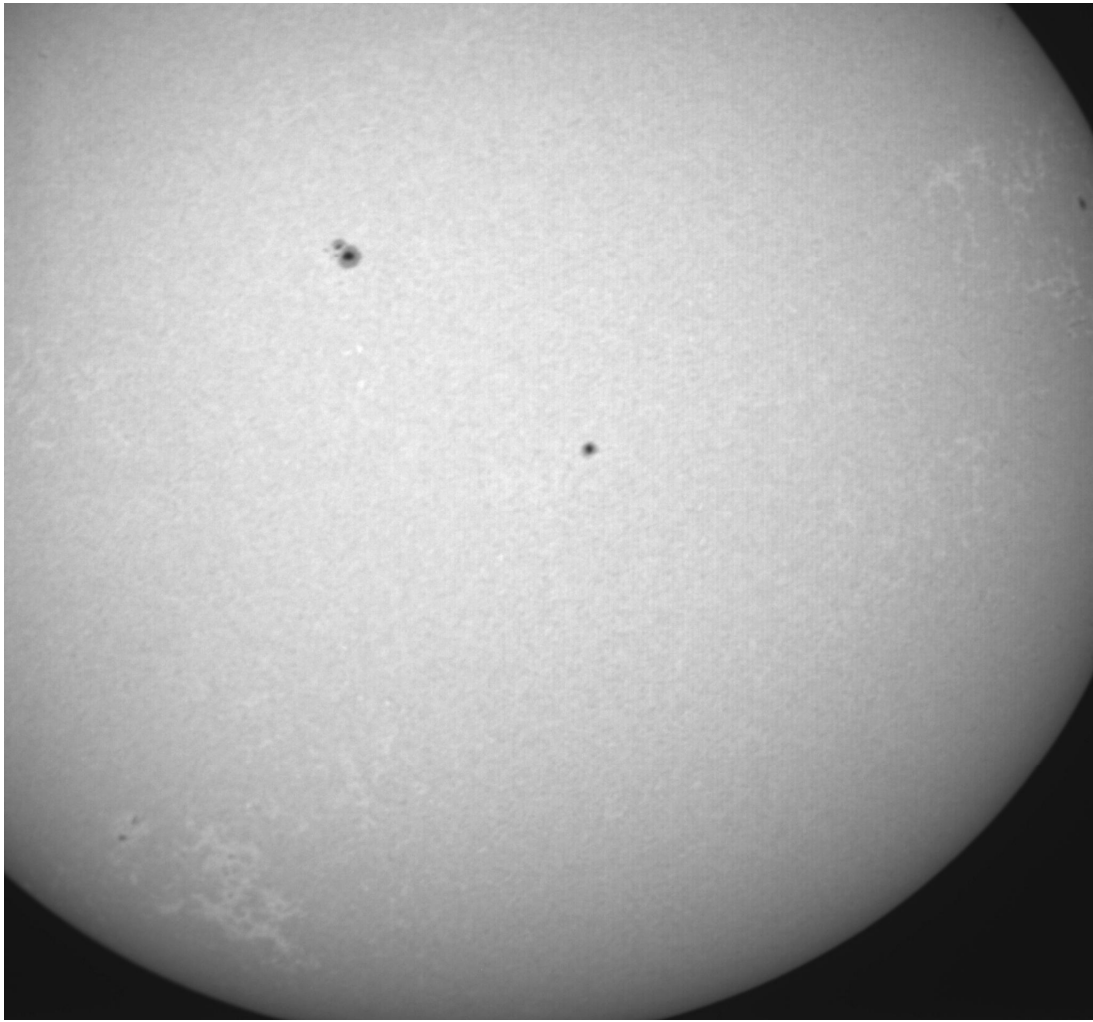


Fig-4: Corrected image by Flat-fielding technique

### **Comparison with SDO**

Helioseismic and Magnetic Imager on-board Solar Dynamic Observatory (SDO/HMI) obtains the photospheric images in the continuum of 617.3 nm line of Fe I. The spatial resolution of the image is 0.5 arc sec per pixel. This is close to the pixel resolution of our G-band images obtained at Merak. SDO/HMI obtains the photospheric images at every 45 sec. In Figure 5 we compare our data having small FOV with the same FOV of SDO/HMI. A comparison shows that the sunspot has very good contrast in the SDO/HMI compared to the G-band observations made from ground based observations. However, the contrast of the background structures is better in the G-band image compared to SDO/HMI. A few small pores near the sunspot (top portion in Figure 5) are seen in SDO images and

are not visible in the G-band images. This could be due to the Earth's atmospheric seeing which smear/blur the image.

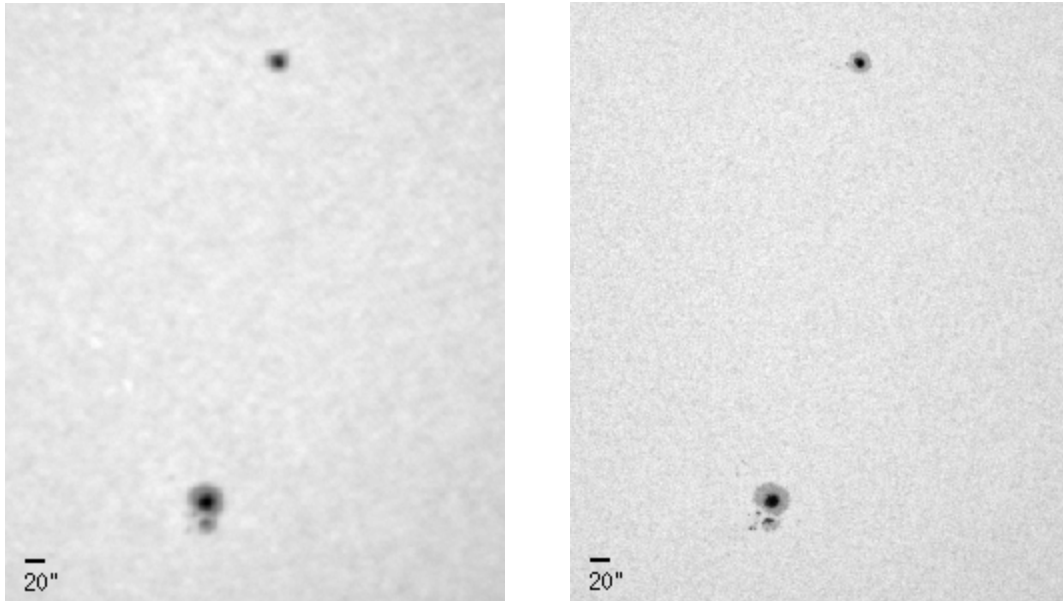


Fig-5: The Left image is the selected portion of our flat fielded image and compared with same region of SDO/HMI continuum image (right image). Active regions seen in the images are NOAA 11375 ( top) and NOAA 11374 (bottom). The flat fielded image is rotated and cropped for comparison with SDO image of same resolution .

In order to quantitatively estimate the spatial resolution obtained, G-band bright points (GBP) were identified. Though it was difficult to identify isolated GBP, clusters of GBP can be easily identified. We chose a cluster where three GBPs are close to each other and were organized in such a way that two of them are aligned in the vertical direction of the image. Figure 6 shows the cluster identified. A vertical cut along the center of these two GBPs provide a way to identify the sizes of the structure assuming a Gaussian intensity profile for both. A two Gaussian function fitting was carried out and estimated the FWHM of individual GBP. Figure 7 shows the intensity profile of the vertical cut as well as the fitted two-Gaussian function and the associated FWHM. The estimated FWHM of these two GBPs are  $3.1''$

and  $4.6''$  with an error of  $\pm 0.1''$ . Hence, the obtained spatial resolution with this setup is better than  $3.2''$ .

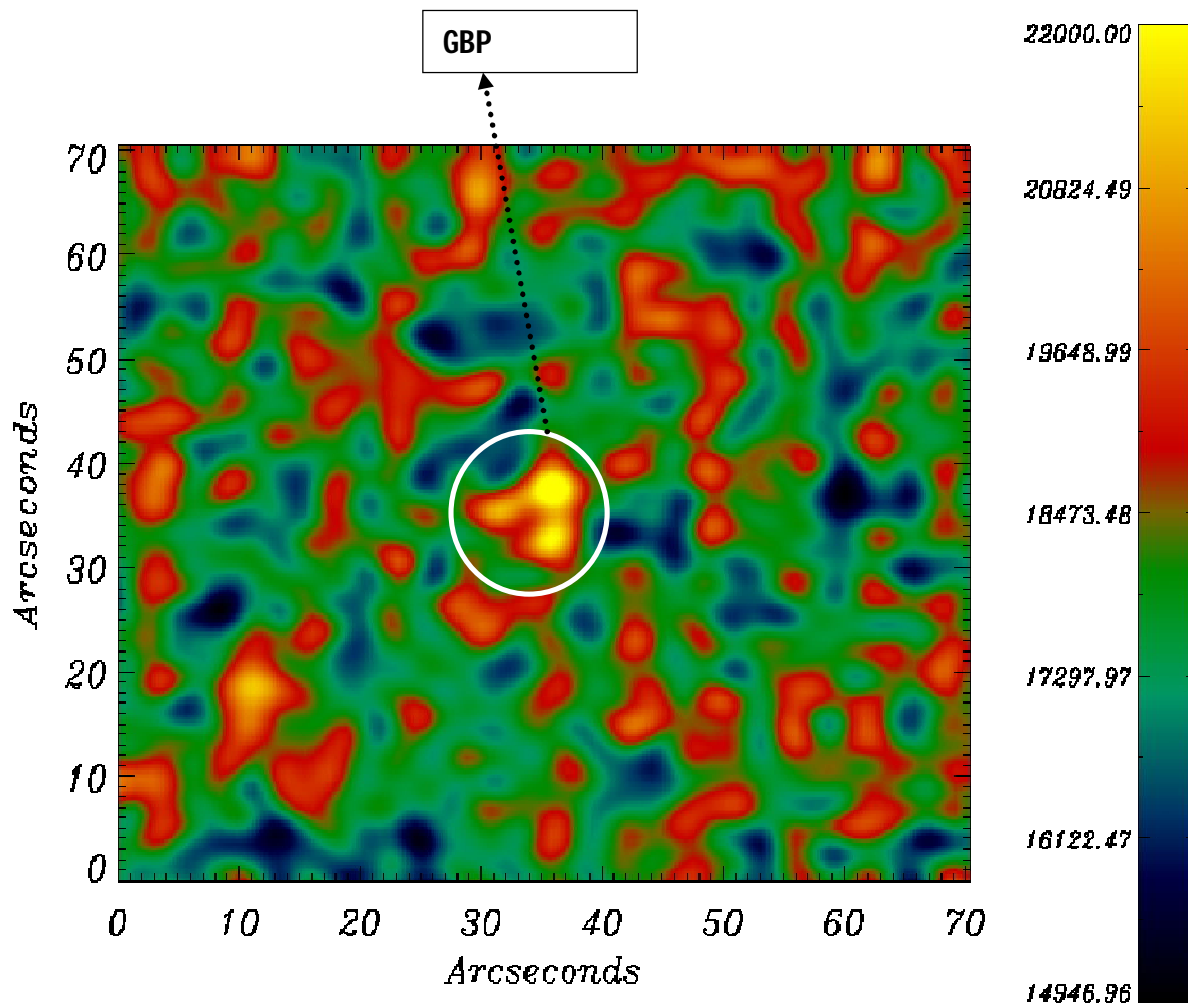


Fig-6: A portion of the observed G-band image to illustrate the clustering of GBPs. This cluster is used to estimate the spatial resolution obtained with this telescope setup.

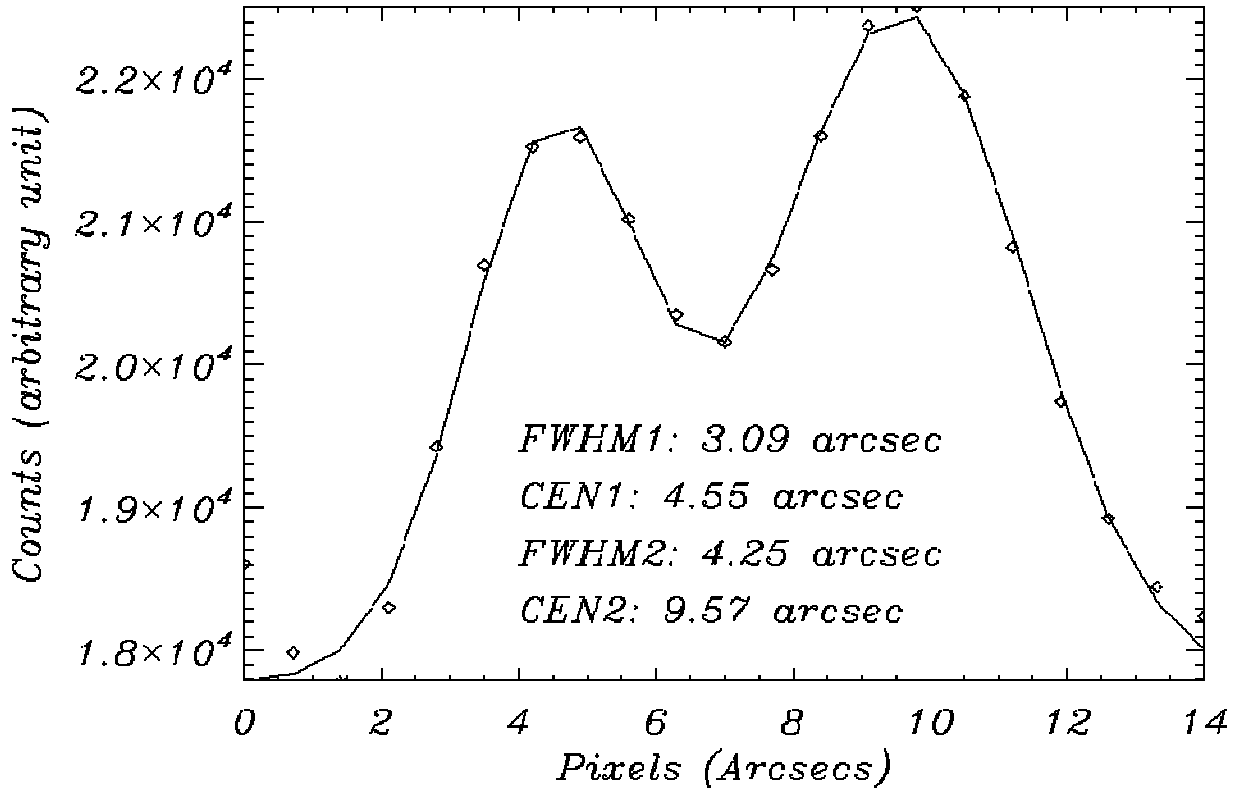


Fig-7: A vertical cut (diamond points) of the GBP cluster and two Gaussian fit (solid line). The estimated FWHM of the two Gaussian fit is also marked in this figure

### Center to Limb Variation of Intensity

The photospheric images exhibits limb darkening effect. The intensity in the center of the image is large compared to the limb. A good calibrated image should show the limb darkening effect. Figure 8 shows the profile of center to limb intensity at three locations on the Sun including quiet as well as active regions. In all these curves, the limb darkening effect is easily seen and the intensity varies smoothly from center to the limb. A shallow dip in the black curve represents the sunspot location which suggests that there is a high contrast between the sunspot and the surrounding region.

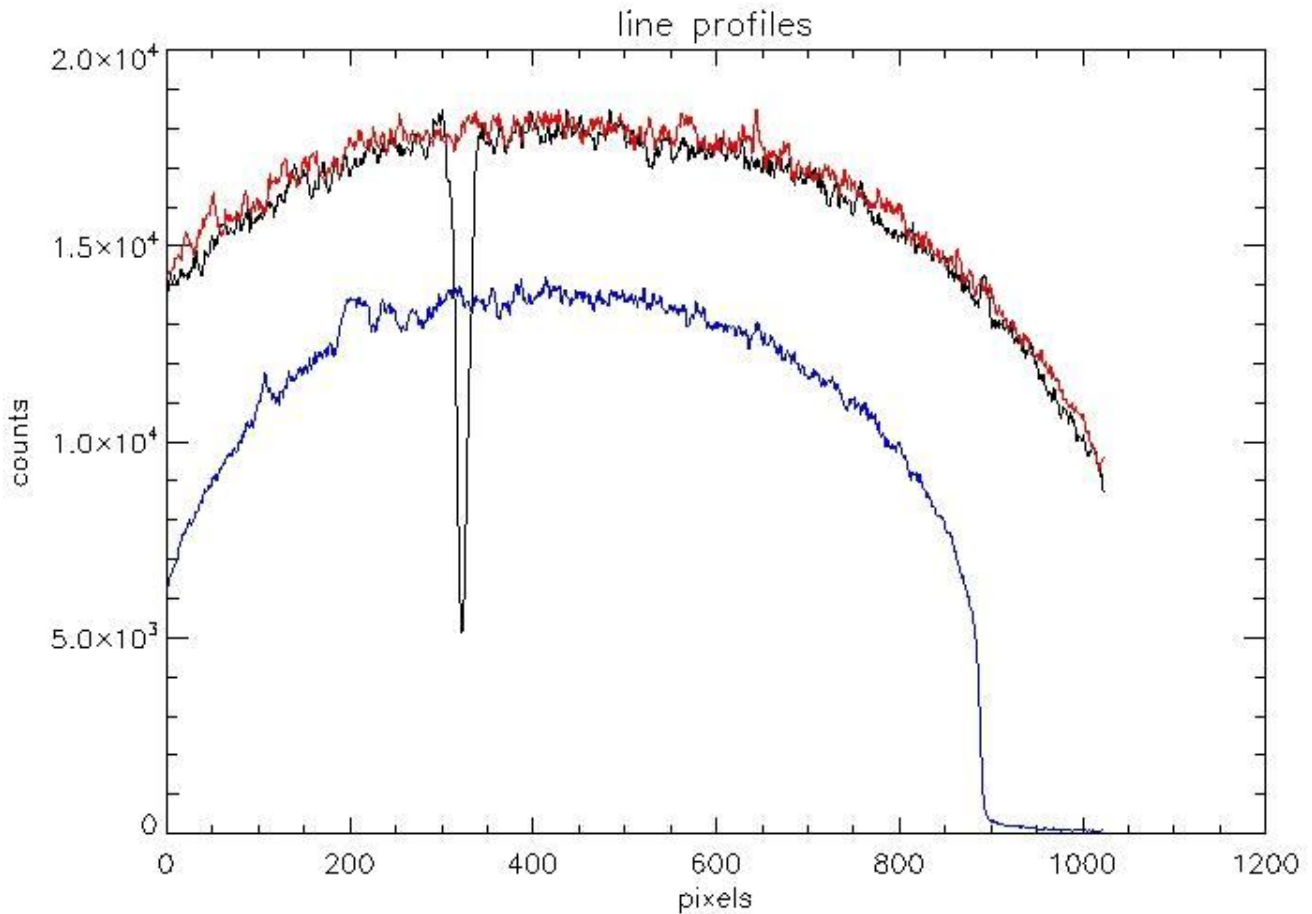


Fig-8: Horizontal line profiles of three different regions in the flat fielded image (re-binned to  $1024 \times 1024$ ) comprising of sunspot, quiet region and plages. Black profile corresponds to the line which passes through sunspot NOAA 11374. Red profile corresponds to quiet region between the sunspots and blue profile corresponds to line which pass through left bottom plage in Fig-4.

Limb darkening profile can be used to identify the scattered light in system that includes the telescope and atmosphere. First we computed the theoretical limb darkening profile for the central wavelength of 430.5 nm with a band pass of 0.8 nm. The theoretical limb darkening profile is computed by using the table given in Astrophysical Quantities edited by Allen (1973). The obtained theoretical curve has been compared with the observed limb darkening curve and is shown in Figure 9. In the plot, the solid line corresponds to the theoretical profile and the dashed line corresponds to the observed limb darkening profile. A close matching of the two suggests that the goodness of the calibration and also the low scattered light level in the telescope.

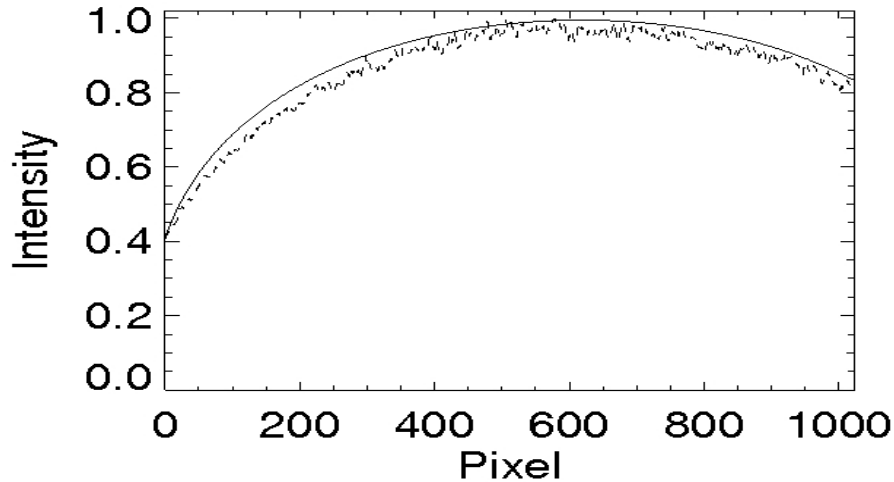


Fig-9: The observed limb darkening profile (dashed curve) is fitted with the theoretical limb darkening profile (solid curve).

## Discussions and Future Plan

One of the main aims of this project is to observe the solar atmosphere in different wavelength bands with moderate sized telescope. This exercise will provide hands on experience to build more sophisticated and complicated instruments for larger telescope such as National Large Solar Telescope (NLST). This also provides a platform to develop the technique to calibrate and analyze the data. In the first stage, we were able to get good images of the Sun in G-band (with an estimated spatial resolution better than  $3.2''$ ), though it is not at very high resolution. The poor resolution is due to the limitation of the instruments and the observational set up. For example, the photo film that we used in front of the tube may be affecting the image quality. We compared the data with the space based data which is already available for the same day. While the results are promising, still we need to improve upon many things. First we need to extend the beam to get the better resolution, close to  $0.3$  arc sec at G-band wavelength. This can be achieved with a good lens which can magnify the image and by using the faster CCD camera. In future we may also use the speckle

reconstruction technique to achieve the diffraction limited images. We can also replace the mylar film with a broad band glass filter so that the film filter does not affect the image quality. There is a proposal to do night time observations to ascertain the capabilities of the system to obtain good images. The observations after the changes in the setup will be reported in the future.

### **Acknowledgement**

We would like to thank Mr. Angchuk Dorje, Tsewang, K. Ravi and Merak team for various help during the installation of the telescope. We also would like to thank Prof. Jagdev Singh who helped us during the initial stages of the project. We are grateful to Prof. Hasan, The Director, IIA for providing the support and encouragement. We are indebted to Prof. K. B. Ramesh for loaning out the PCO camera and reading the manuscript. Mr. Kemkar, Mr. V. K. Subramanian and the IIA workshop team designed and fabricated the mechanical adapters used with the telescope. We also thank the referee for the critical comments that gives an opportunity to improve the observational setup in the future.

### **References:**

1. Ishikawa, R., Tsuneta, S., Kitakoshi, Y. et al. 2007, *A&A*, 472, 911.
2. Vögler, A., & Schüssler, M. 2003, *Astron. Nachr./AN*, 324, 399
3. Langhans, K., Schmidt, W., & Tritschler, A. 2002, *A&A*, 394, 1069
4. Rutten, R. J., Hammerschlag, R. H., Sütterlin, P., & Bettonvil, F. C.M. 2001, in *Advanced Solar Polarimetry – Theory, Observation, and Instrumentation*, ed. M. Sigwarth (San Francisco: Astron. Society of the Pacific), ASP Conf. Ser., 236, 25.
5. Sánchez Almeida, J., Asensio Ramos, A., Trujillo Bueno, J., & Cernicharo, J. 2001, *ApJ*, 555, 978
6. Berger, T. E., & Title, A. M. 1996, *ApJ*, 463, 365.
7. Berger, T. E., Schrijver, C. J., Shine, R. A., Tarbell, T. D., Title, A. M., Scharmer, G., 1995, *ApJ*, 454, 531.
8. Spruit, H. C. 1976, *Sol. Phys.*, 50, 269